Am J Transl Res 2020;12(5):2155-2168
www.ajtr.org /ISSN:1943-8141/AJTR0104716

Original Article

Long noncoding RNA AFAP1-AS1 promotes osteosarcoma progression by regulating miR-497/IGF1R axis

Dan Fei[1*], Xiaona Zhang[3*], Yang Lu[1], Long Tan[1], Mingzhu Xu[2], Yang Zhang[4]

Departments of [1]Ultrasonographic, [2]Nephrology, The Third Hospital of Jilin University, Changchun 130033, P. R. China; Departments of [3]Anesthesiology, [4]Neurosurgery, The First Hospital of Jilin University, Changchun 130021, P. R. China. [*]Equal contributors.

Received November 10, 2019; Accepted May 5, 2020; Epub May 15, 2020; Published May 30, 2020

Abstract: Long non-coding RNA (lncRNA) actin filament-associated protein 1 antisense RNA 1 (AFAP1-AS1) has been reported to be involved in the progression of multiple cancers. However, exact function and regulatory mechanism of AFAP1-AS1 in osteosarcoma (OS) remain largely unclear. In this study, quantitative real time polymerase chain reaction (qRT-PCR) revealed that AFAP1-AS1 was upregulated in OS tissues and cell lines. Increased AFAP1-AS1 was associated with poor prognosis. Loss-of-function experiments demonstrated that knockdown of AFAP1-AS1 inhibited the proliferation, colony formation, migration, invasion and induced cell apoptosis. Bioinformatics analysis and luciferase reporter assays confirmed that mircoRNA-497 (miR-497) was a directly target of AFAP1-AS1. Rescue experiments confirmed that miR-497 inhibition could partially reverse the inhibitory effect of AFAP1-AS1 knockdown on OS cells. Moreover, AFAP1-AS1 modulated the expression of insulin-like growth factor 1 receptor (IGF1R, a target of miR-497) indirectly. *In vivo* xenograft tumor assay showed that AFAP1-AS1 knockdown inhibited tumor tumorigenesis. Taken together, these findings indicate that AFAP1-AS1 promotes OS progression by regulating miR-497/IGF1R axis, providing a therapeutic target for OS.

Keywords: LncRNA, osteosarcoma, AFAP1-AS1 miR-497, IGF1R

Introduction

Osteosarcoma (OS) is a common malignant bone cancer among adolescents and children under the 20 years of age [1]. Despite advances in the treatment of OS in surgery, chemotherapy and biologics in recent years, the survival rate in patients remains very low because of its characteristic early metastasis [2, 3]. Therefore, understanding of the underlying mechanisms associated with OS progression is urgent need to improve current therapeutic approaches for OS.

Long non-coding RNAs (lncRNAs) and microRNAs (miRs) have been largely gained attention in cancer study, and might become new opportunities for cancer diagnosis and treatment [4-7]. Emerging studies have showed that both lncRNAs and miRs were involved in carcinogenesis, invasion, and metastasis of various cancers [8, 9]. Recently, a range of lncRNAs and miRNAs were identified to participate in initiation and development of OS, functioning as oncogenes or tumor suppressors [10-12].

LncRNA actin filament associated protein 1 antisense RNA1 (AFAP1-AS1), a new discovery lncRNA, was reported to be upregulated, and played an oncogenic role in multiple types of cancers [13], such as nasopharyngeal carcinoma [14], pancreatic ductal adenocarcinoma [15], non-small cell lung cancer [16], glioma [17], breast cancer [18], colorectal cancer [19], and thyroid cancer [20]. Although AFAP1-AS1 was found to be upregulated in OS tissues [21, 22], the functional involvement of AFAP1-AS1 in OS remains largely unclear.

MiR-497, an important miR, has been reported to be downregulated, and function as tumor suppressor in many cancers by regulating cancer cell proliferation, invasion, apoptosis, metastasis, and so on [23]. For OS, miR-497 ex-

Table 1. Correlation between clinicopathological features and AFAP1-AS1 expression in 45 patients with OS

Variables	No. of cases	AFAP1-AS1 expression		*P* value
		High	Low	
Age (years)				*P* = 0.9875
< 20	31	17	14	
≥ 20	14	7	7	
Gender				*P* = 0.7775
Male	25	13	12	
Female	20	11	9	
TNM stage				*P* < 0.001
I-II	36	15	21	
III-IV	9	9	0	
Tumor size				*P* = 0.0094
< 5 cm	32	13	19	
≥ 5 cm	13	11	2	
Metastasis				*P* = 0.0115
No	35	15	20	
Yes	10	9	1	

pression was downregulated, and functioned as a tumor suppressor [24, 25]. Interestingly, in the study, we found that there was an interaction between miR-497 and AFAP1-AS1 through the bioinformatic analysis (Starbase2.0). Thus, we examined the expression of AFAP1-AS1 in OS tissues and cell lines to investigate its clinical significance. We also investigated the role of AFAP1-AS1 in the progression of OS in *vitro* and *in vivo* on basis of a series of experiments.

Materials and methods

Clinical specimens

Total 45 patients with OS that have never received therapy prior to surgery were recruited from the Third Hospital of Jilin University (Changchun, China) in present study. All samples were collected after acquirement of informed consent from all patients, and rapid frozen in liquid nitrogen and stored at -80°C for qRT-PCR analysis. All patient characteristics are presented in **Table 1**. All protocols were approved by Ethics Committee of the China-Japan Union Hospital of Jilin University.

Cell culture and transfection

OS cell lines (MG-63, 143B, U2OS, Saos-2) and normal human osteoblasts hFOB 1.19 cells were purchased from the Cell Bank of the Chinese Academy of Sciences (Shanghai, China). All cells were maintained in Dulbecco's modified Eagle's medium (DMEM; Gibco, Grand Island, NY, USA) supplemented with 10% fetal bovine serum (FBS; Gibco) and 1% penicillin-streptomycin (Invitrogen, CA, USA) in incubator (37°C, 5% CO_2).

Three hairpin (sh)RNAs targeting AFAP1-AS1 (sh-AFAP1-AS1#1, sh-AFAP1-AS1#2, and sh-AFAP1-AS1#3) and non-target shRNA control (sh-NC) were designed and synthesized from ObiO (Shanghai, China), and inserted into the GV248 vector (Genechem, Shanghai, China). Stable clones with sh-AFAP1-AS1 were selected for 4 weeks using puromycin. MiR-497 inhibitors (miR-497 in), miR-497 mimics and corresponding negative control (miR-NC, anti-miR-NC) were bought from Genecopoeia (Guangzhou, China). U2OS cells were transfected with above-mentioned molecules production using Lipofectamine™ 2000 reagent (Invitrogen) according to the instructions. After transfection for 48 hours (h), the samples were collected and transfection efficiency was examined by qRT-PCR.

RNA isolation and qRT-PCR analysis

Total RNA from tissues specimens and cultured cells was insolated using Trizol reagent (Invitrogen) following the manufacturer's protocol. Reverse transcription was performed according to the protocol of PrimeScriptTM RT Master Mix Kit (Takara, Japan) and Mir-X miRNA qRT-PCR SYBR Kit (Takara). Quantitative real time PCR (qRT-PCR) was performed using SYBR Premix Ex Taq™II (Takara) on a 7500 Fast Real-Time PCR System (Applied Biosystems, USA). U6 and glyceraldehyde-3-phosphate dehydrogenase (GAPDH) were used as endogenous controls, respectively. The relative expression levels were calculated using the $2^{-\Delta\Delta Ct}$ method. The primers used in this study were listed in **Table 2**.

Cell proliferation and colony formation assays

For cell proliferation assay, the transfected cells were seeded onto a 96-well plate at density of 5×10^3 cells per well. Cell counting Kit-8 solution (CCK8, Dojindo Molecular

Table 2. Real time PCR primers used for mRNA or miRNA expression analysis

Target gene	Prime (5'-3')
U6	F-TCCGATCGTGAAGCGTTC
	R-GTGCAGGGTCCGAGGT
miR-497	F-AGTCCAGTTTTCCCAGGAATCCCT
	R-ACCAGCAGCACACTGTGGTTTGT
AFAP1-AS1	F-AATGGTGGTAGGAGGGAGGA
	R-CACACAGGGGAATGAAGAGG
IGF1R	F-TTTCCCACAGCAGTCCACCTC
	R-AGCATCCTAGCCTTCTCACCC
GAPDH	F-AAGGTGAAGGTCGGAGTCAA
	R-AATGAAGGGGTCATTGATGG

Abbreviations: F, forward; mRNA, messenger RNA; PCR, polymerase chain reaction; R, reverse.

Technologies, Tokyo, Japan) were added into well at indicated time (0, 24, 48, 72 h). The absorbance at 450 nm was read in a microplate reader (BioTek, Winooski, VT).

For colony formation assay, stable AFAP1-AS1-depleted U2OS cells were incubated in each well of 6-well plates at density of 1000 cells/well. After cultured at 37°C for 10 days, the colonies were fixed with 96% ethanol and stained with 1% crystal violet following manually imaged and counted using an inverted microscope (Olympus Corporation, Tokyo, Japan).

Cell apoptosis assay

Cells were collected at 48 h post-transfection. Apoptosis was detected using Annexin V Apoptosis Detection Kits (Becton Dickinson, San Jose, CA, USA) under flow cytometer FACS Calibur (Becton Dickinson). The apoptosis ratio was analyzed by FACS Diva (Becton Dickinson).

Cell migration and invasion assays

Cell migration was determined by wound healing assay. Briefly, transfected cells were seed in 6-well plates. Upon reaching 100% confluence, the cell layer was gently and slowly scratched to create wound using a pipette tip. After washing with PBS, the cells were cultured in free-serum medium for 24 h. Wound closure was imaged at 0 and 24 h after scratched. The wound area was analyzed by Image J software (NIH, Bethesda, MD, USA).

Cell invasion assay was carried out using 24-well transwell chambers (pore size 8 μm; Corning, Inc., Corning, NY, USA). Briefly, the transfected cells were seeded on the upper membrane pre-coated with Matrigel (BD, Franklin Lakes, NJ, USA) in free-serum medium, the lower chamber was filled with medium containing 10% FBS as a chemoattractant. After incubation at 37°C for 48 h, the invaded cells were fixed with 4% paraformaldehyde for 20 min and stained with 1% crystal violet for 15 min. Invaded cells were photographed and counted in five randomly selected visual fields of each insert under a light microscope at 200 × magnification.

Luciferase activity assay

The miRs that target AFAP1-AS1 were identified using the Starbase2.0 software (http://starbase.sysu.edu.cn/starbase2/mirLncRNA.php). The wild-type (WT) or mutant (MUT) AFAP1-AS1 binding sites of miR-497 was synthesized and inserted into a pGL3 basic vector (Promega, Madison, WI, USA), represented as WT-AFAP1-AS1 and MUT-AFAP1-AS1, respectively. For luciferase reporter assay, U2OS cells were transfected with miR-497 mimics or miR-NC mimics, along with and WT-AFAP1-AS1 or MUT-AFAP1-AS1 reporter plasmid. At 48 h post-transfection, renilla luciferase and firefly luciferase activities were determined using the dual-luciferase reporter assay system (Promega). Luciferase activity was normalized to Renilla luciferase activity.

RNA immunoprecipitation (RIP) assay

RIP assay was conducted using an EZ-Magna RIP RNA-binding protein immunoprecipitation kit (Millipore Corp., Billerica, MA, USA) following the manufacturer's instructions. U2OS cells were lysed by RIP lysis buffer (Millipore Corp) and incubated with magnetic beads conjugated with normal mouse IgG (as control) or human anti-Ago2 antibody (Abcam, Cambridge, MA, USA). Purified RNA was isolated and subjected to qRT-PCR to detection of AFAP1-AS1 and miR-497.

Western blot analysis

Total proteins were isolated from cultured cells using RIPA Buffer (Pierce, Rockford, IL, USA). Concentrations of total protein were measured

using a BCA assay kit (Beyotime, Biotechnology, Shanghai, China). Total protein samples (30 μg) was electrophoresed with SDS-polyacrylamide gel electrophoresis, and transferred to the PVDF membrane (Merck Millipore, MA, USA). After blocked with 5% non-fat milk, the membrane was incubated with primary antibody against IGF1R (1:1000 dilution; Abcam, CA, USA) and GAPDH (1:3000 dilution; Abcam) at 4°C overnight. Subsequently, membrane was washed and incubated with secondary antibodies (1:5000 dilution; Abcam). The protein bands were observed using enhanced chemiluminescence (ECL) kit (GE Healthcare, Freiburg, DE).

In vivo experiments

Ten male athymic 4-week-old BALB/c nude mice were obtained from the Central Laboratory of Animal Science of Jilin University (Changchun, China). All experimental procedures about animal were approved by the Institutional Animal Care and Use Committee of the Jilin University (Changchun, China).

All mice were randomly divided into two groups and received 2×10^6 U2OS cells stably transfected with sh-AFAP1-AS1 and sh-NC via subcutaneously injected, respectively. Tumor volume was measured every 5 days until the mice were sacrificed. The tumor volume was calculated using the following formula: tumor volume (mm^3) = (length × $width^2$)/2. 30 days after injection, the mice were sacrificed, the tumor were removed and weighted. A part of tumor tissues were paraffin-embedded, and formalin-fixed, followed by immunostaining for Ki-67 expression. Other part of tumor tissues were stored at -80°C until use.

Immunohistochemistry (IHC)

IHC were conducted to detect Ki-67 expression as described previously [26]. Ki-67 primary antibody (Abcam) and the biotinylated secondary antibody (ZSGB-BIO, Beijing, China) were used in this study.

Statistical analysis

The SPSS 18.0 software (SPSS Inc., Chicago, IL) was applied to do statistical analysis. Student's t test or one-way analysis of variance was used to analyze the difference among/between sample groups. The relationship between AFAP1-AS1 and clinicopathologic characteristics of patients was determined using χ^2 test. Pearson's correlation coefficient analysis was used to analyze the correlations. Survival curves were plotted using the Kaplan-Meier method and were analyzed using a log-rank test. Difference with $P < 0.05$ was considered as statistically significant.

Results

Up-regulation of AFAP1-AS1 was correlated with clinical outcome and prognosis in patients with OS

To investigate roles played by AFAP1-AS1 in OS, the expression of AFAP1-AS1 was examined in four human OS cell lines (MG-63, 143B, U2OS, Saos-2) and normal human osteoblasts hFOB 1.19 cells. The expression of AFAP1-AS1 was higher in four OS cell lines than that of hFOB 1.19 cells (**Figure 1A**). Furthermore, we detect the expression of AFAP1-AS1 in 45 pairs of OS tissues and adjacent normal tissues. qRT-PCR assay revealed that the expression of AFAP1-AS1 was significantly increased in OS tissues compared to adjacent normal tissues (**Figure 1B**).

To verify the association between AFAP1-AS1 expression and the clinical significance in patients with OS, the patients were divided into two groups: AFAP1-AS1 high expression (n = 24) and AFAP1-AS1 low expression groups (n = 21) based on mean of the expression levels. The results showed that AFAP1-AS1 expression was closely associated with tumor size, metastasis, and tumor-node-metastasis (TNM) stage (**Table 1**). Kaplan-Meier analysis revealed that patients with high AFAP1-AS1 levels had poor overall survival rate compared to patients with low AFAP1-AS1 expression level (**Figure 1C**). Collectively, these results implied that AFAP1-AS1 might play an oncogenic role in the development of OS.

AFAP1-AS1 knockdown decreased the proliferation and induced apoptosis of OS cells

To investigate the biological function of AFAP1-AS1 in OS, we decreased the expression of AFAP1-AS1 in U2OS cells by transfection of three shRNAs against AFAP1-AS1 (#1, #2 and #3). As shown in **Figure 2A**, three shRNAs all

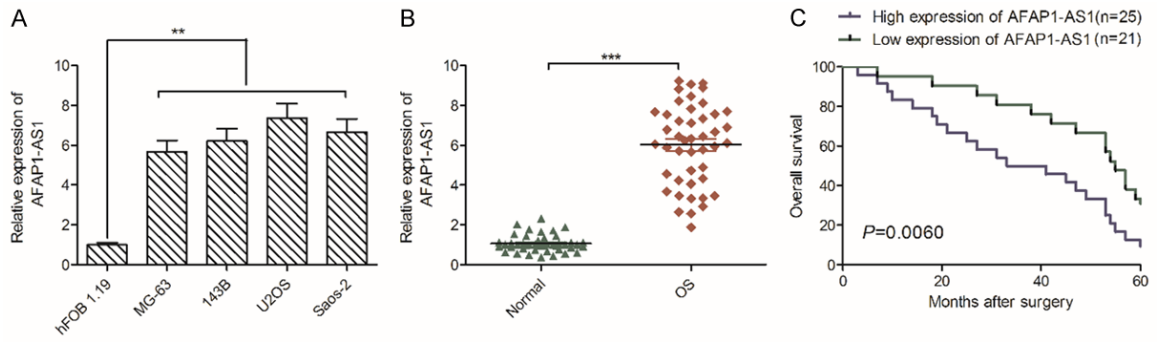

Figure 1. The AFAP1-AS1 expression was upregulated in OS tissues and cell lines. A. The expression of AFAP1-AS1 was upregualted in four human OS cell lines (MG-63, 143B, U2OS, Saos-2) compared with normal human osteoblasts hFOB 1.19 cells. B. The expression of AFAP1-AS1 was upregulated in human OS tissues compared with adjacent normal tissues. C. High expression of AFAP1-AS1 had poor overall survival ration for patients with OS. Data were presented as mean ± standard deviation (SD). Each experiment was repeated three times. $^{**}P < 0.01$, $^{***}P < 0.001$.

significantly decreased AFAP1-AS1 expression in U2OS cells. Among sh-AFAP1-AS1#2 exhibited the lowest expression of AFAP1-AS1 in three plasmids, thus, sh-AFAP1-AS1#2 was chosen for subsequent experiments, and named as sh-AFAP1-AS1. A then CCK8, plate clone formation and flow cytometry assays were conducted to assess the effects of on cell proliferation, colony formation and apoptosis in OS cells, respectively. The results revealed that knockdown of AFAP1-AS1 significantly inhibited cell proliferation, colony formation and promoted apoptosis of U2OS cells (**Figure 2B-D**).

AFAP1-AS1 knockdown decreased the migration and invasion of OS cells

We next investigated the effect of AFAP1-AS1 on migration and invasion of OS cells by wound healing and tranwells invasion assays, respectively. Our results revealed that AFAP1-AS1 knockdown obviously suppressed the migration and invasion of U2OS cells (**Figure 3A** and **3B**).

MiR-497 can serve as a direct target of AFAP1-AS1 in OS cells

The potential targeting miRs binding with AFAP1-AS1 were screened using Starbase2. There were a putative binding site between AFAP1-AS1 and miR-497 (**Figure 4A**). In addition, we found that miR-497 expression was significantly downregulated in OS cell lines and tissues ($P < 0.01$, **Figure 4B** and **4C**). Pearson correlation analysis indicated that AFAP1-AS1 expression was negatively correlated with miR-497 expression in OS tissues ($r = -0.518$, $P < 0.001$, **Figure 4D**). Furthermore, luciferase reporter assay revealed that miR-497 overexpression significantly decreased the luciferase activity of WT-AFAP1-AS1, rather than of MUT-AFAP1-AS1 in U2OS cells (**Figure 4E**). Then anti-Ago2 RNA immunoprecipitation (RIP) assay demonstrated that both AFAP1-AS1 and miR-497 were enriched in pulled down Ago2 protein in U2OS cells (**Figure 4F**). In addition, qRT-PCR results revealed that miR-497 expression was increased in U2OS cells transfected with sh-AFAP1-AS1 (**Figure 4G**), whereas the expression of AFAP1-AS1 was decreased in U2OS cells transfected with miR-497 mimics (**Figure 4H**). These results suggested that miR-497 was a downstream target of AFAP1-AS1 in OS cells.

MiR-497 inhibition reversed the inhibitory effects of AFAP1-AS1 knockdown in OS cells

Next, we performed rescue experiments to explore whether miR-497 mediated the effects of AFAP1-AS1 on cell proliferation, apoptosis, migration and invasion in OS cells. qRT-PCR analysis revealed that miR-497 inhibitor decreased the expression of miR-497 induced by sh-AFAP1-AS1 in U2OS cells (**Figure 5A**) Rescue experiments demonstrated that miR-497 inhibitor reversed the effect of sh-AFAP1-AS1 on cell proliferation, colony formation, apoptosis, migration and invasion in U2OS cells (**Figure 5B-F**). These results implied that AFAP1-AS1 exerted tumor-promoting role in OS cells partially regulating miR-497.

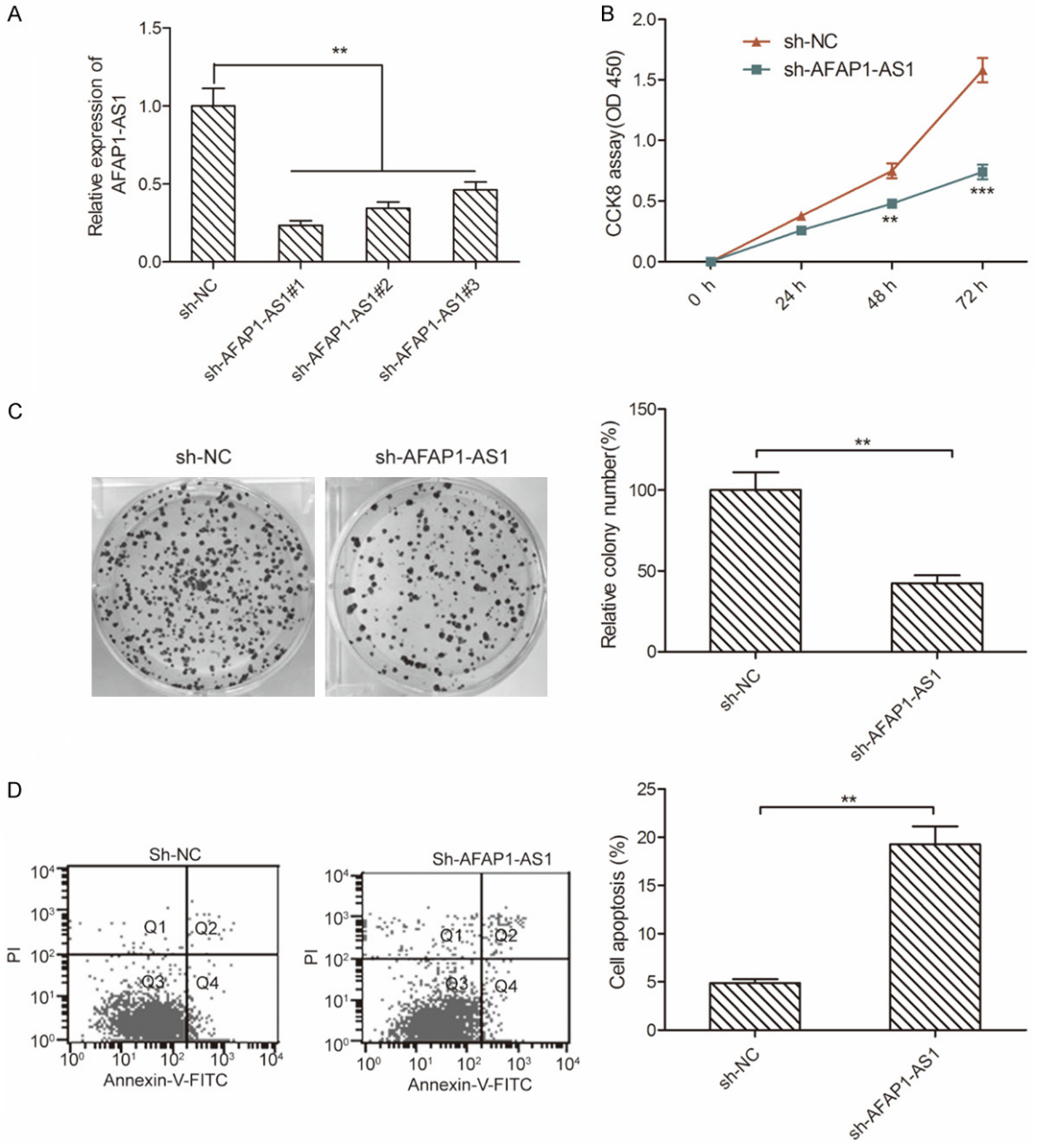

Figure 2. AFAP1-AS1 knockdown decreased the proliferation and cell cycle of OS cells. A. The expression of AFAP1-AS1 was downregulated in U2OS cells transfected with sh-AFAP1-AS1 or sh-NC by qRT-PCR. B. CCK8 assay revealed that AFAP1-AS1 knockdown inhibited cell proliferation in U2OS cells. C. AFAP1-AS1 knockdown inhibited colony formation of U2OS cells. D. Flow cemetery assay demonstrated that AFAP1-AS1 knockdown induced cell apoptosis of U2OS cells. Data were presented as mean ± standard deviation (SD). Each experiment was repeated three times. $*P < 0.05$, $**P < 0.01$.

Associated role of AFAP1-AS1, miR-497 and IGF1R in OS progression

LncRNAs could serve as endogenous sponges or ceRNAs by inhibiting subsequent miRs binding to target mRNAs [27]. Previous a study showed that miR-497 could target IGF1R to inhibit OS progression [23]. Here, we investigated the association AFAP1-AS1, miR-497 and IGF-1R in OS. We found that knockdown of AFAP1-AS1 inhibited IGF1R mRNA and protein expression levels, while miR-497 inhibitor could par-

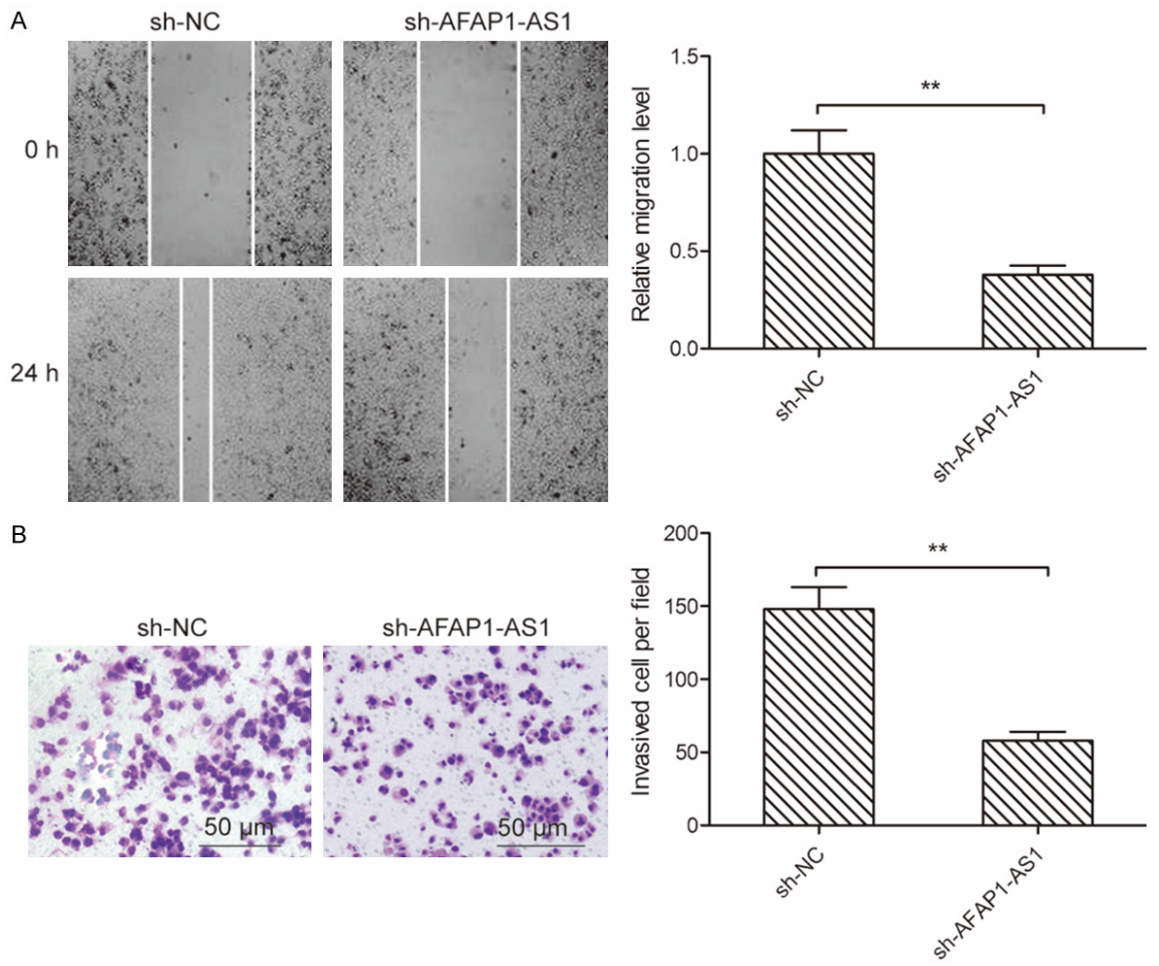

Figure 3. AFAP1-AS1 knockdown suppressed the migration and invasion of OS cells. A. Wound healing assay showed that AFAP1-AS1 knockdown suppressed migration of U2OS cells. B. Transwell invasion assay demonstrated that AFAP1-AS1 knockdown suppressed invasion of U2OS cells. Data were presented as mean ± standard deviation (SD). Each experiment was repeated three times. $^{**}P < 0.01$.

tially AFAP1-AS1 expression in U2OS cells (**Figure 6A** and **6B**). Moreover, we found that *IGF-1R* mRNA expression levels were upregulated in OS cell lines and tissues (**Figure 6C** and **6D**). Pearson correlation analysis indicated that *IGF1R* expression was negatively correlated with miR-497 expression in OS tissues (r = -0.622, $P < 0.001$, **Figure 6E**), and positively correlated with AFAP1-AS1 expression in OS tissues (r = 0.563, $P < 0.001$, **Figure 6F**). These data implied that the AFAP1-AS1 could regulate IGF1R expression by sponging miR-497 in OS.

Knockdown of AFAP1-AS1 inhibited tumor growth in vivo

To investigate the role of AFAP1-AS1 on OS growth *in vivo*, we conducted a xenograft model experiment. We found that the tumor growth was slower in sh-AFAP1-AS1 group than that of sh-NC group (**Figure 7A**). At the end of experiments, the mice were killed and tumor tissues were removed and weighted. Results demonstrated that tumor sizes and weights were decreased in in sh-AFAP1-AS1 group compared to the sh-NC group (**Figure 7B** and **7C**). Immunohistochemistry revealed that knockdown of AFAP1-AS1 decreased the proportion of Ki-67-positive cells (**Figure 7D**). In addition, we examined the expression of AFAP1-AS1, miR-497 and IGF1R in xenograft tumor. The results of qRT-PCR showed that knockdown of AFAP1-AS1 decreased AFAP1-AS1 and *IGF1R* expression, and increased miR-497 expression in xenograft tumor tissues (**Figure 7E**). These results suggested that AFAP1-AS1 knockdown suppressed tumor growth *in vivo*.

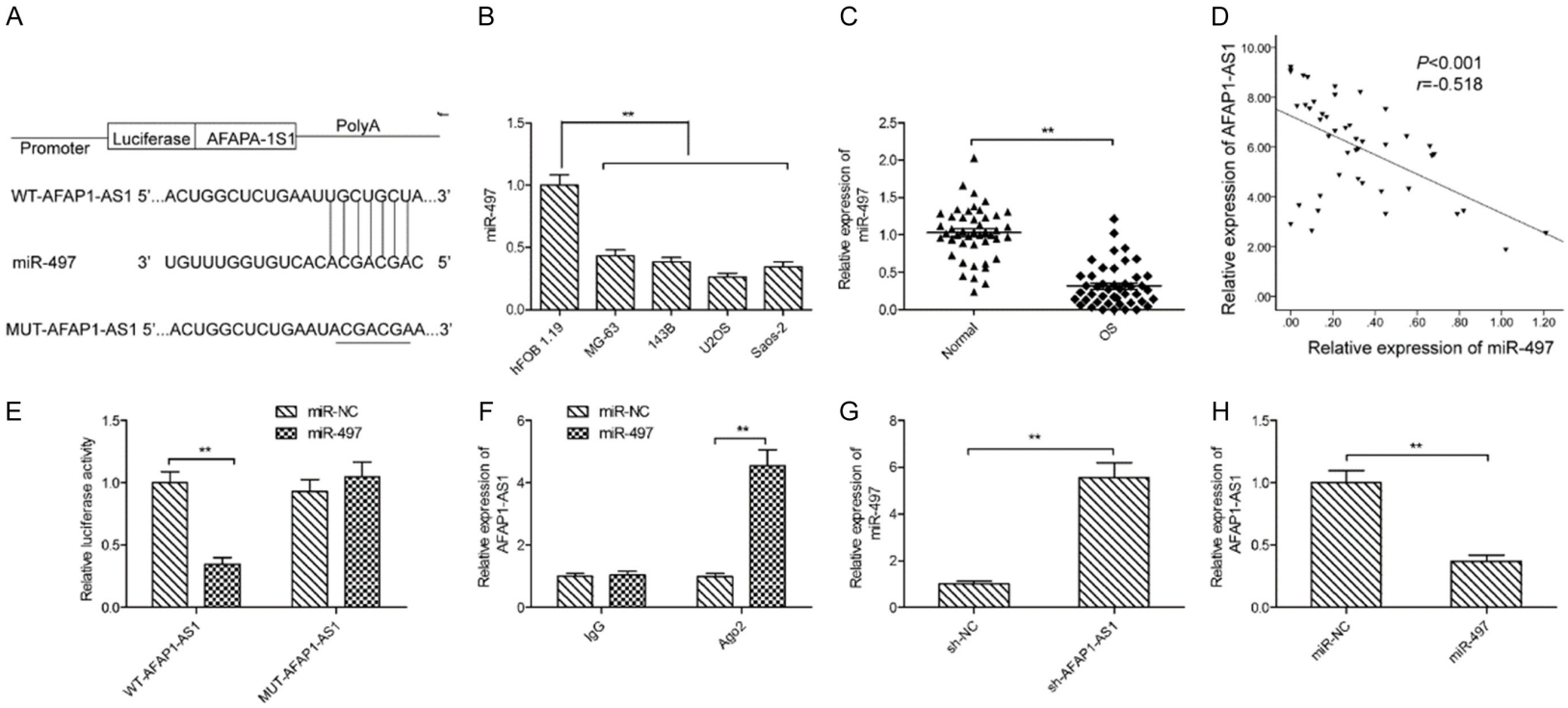

Figure 4. miR-497 could serve as a direct target of AFAP1-AS1 in OS cells. A. The binding sites of AFAP1-AS1 (WT-AFAP1-AS1) and mutants sites (MUT-AFAP1-AS1) were shown. B. The expression of miR-497 was downregulated in four human OS cell lines (MG-63, 143B, U2OS, Saos-2). C. The expression of miR-497 was downregulated in human OS tissues. D. Pearson correlation analysis disclosed that there existed a negative association between miR-497 and AFAP1-AS1 in OS tissues. E. Overexpression of miR-497 decreased luciferase activity of WT-AFAP1-AS1 in U2OS cells. F. The anti-Ago2 RIP assay with miR-497 mimics revealed that both miR-497 and AFAP1-AS1 were enriched in Ago2 precipitate compared to control (IgG) in U2OS cells. G. The expression of miR-497 was increased in U2OS cells transfected with sh-AFAP1-AS1 or sh-NC by qRT-PCR. H. The expression of AFAP1-AS1 was decreased in U2OS cells transfected with miR-NC or miR-497 mimics. Data were presented as mean ± standard deviation (SD). Each experiment was repeated three times. $*P < 0.05$, $**P < 0.01$.

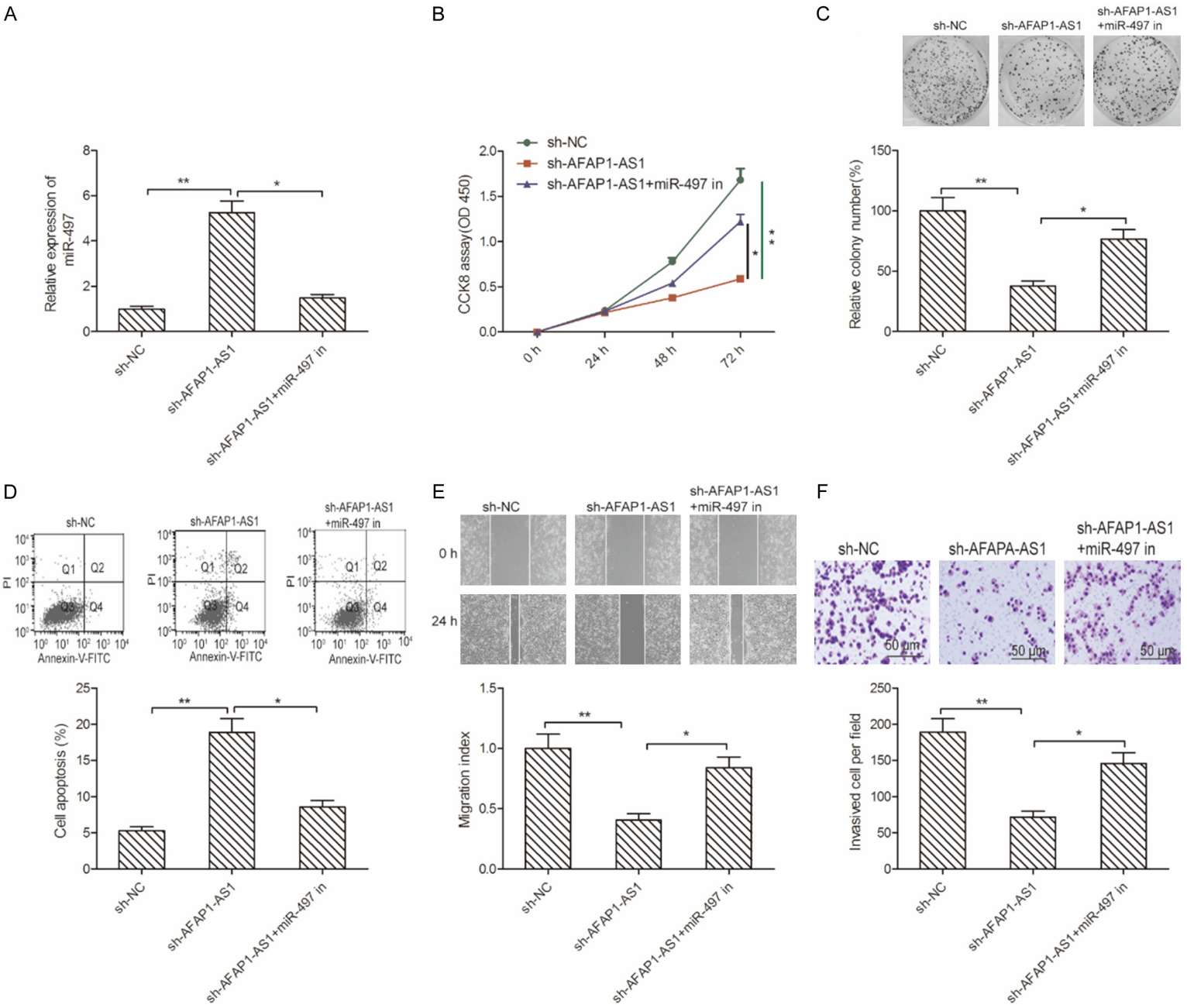
A
Relative expression of miR-497
sh-NC
sh-AFAP1-AS1
sh-AFAP1-AS1+miR-497 in
B
CCK8 assay(OD 450)
sh-NC
sh-AFAP1-AS1
sh-AFAP1-AS1+miR-497 in
0 h
24 h
48 h
72 h
C
sh-NC
sh-AFAP1-AS1
sh-AFAP1-AS1 +miR-497 in
Relative colony number(%)
D
sh-NC
sh-AFAP1-AS1
sh-AFAP1-AS1 +miR-497 in
PI
Annexin-V-FITC
Q1
Q2
Q3
Q4
Cell apoptosis (%)
E
sh-NC
sh-AFAP1-AS1
sh-AFAP1-AS1 +miR-497 in
0 h
24 h
Migration index
F
sh-NC
sh-AFAPA-AS1
sh-AFAP1-AS1 +miR-497 in
50 μm
Invasived cell per field

Figure 5. miR-497 inhibition reversed the inhibitory effects of AFAP1-AS1 knockdown in OS cells. A. miR-497 inhibition reversed the expression of miR-497 mediated by AFAP1-AS1 depletion in U2OS cells. B-F. miR-497 inhibition reversed the effects of AFAP1-AS1 knockdown in U2OS cell proliferation, colony formation, apoptosis, migration and invasion. Data were presented as mean ± standard deviation (SD). Each experiment was repeated three times. *P < 0.05, **P < 0.01.

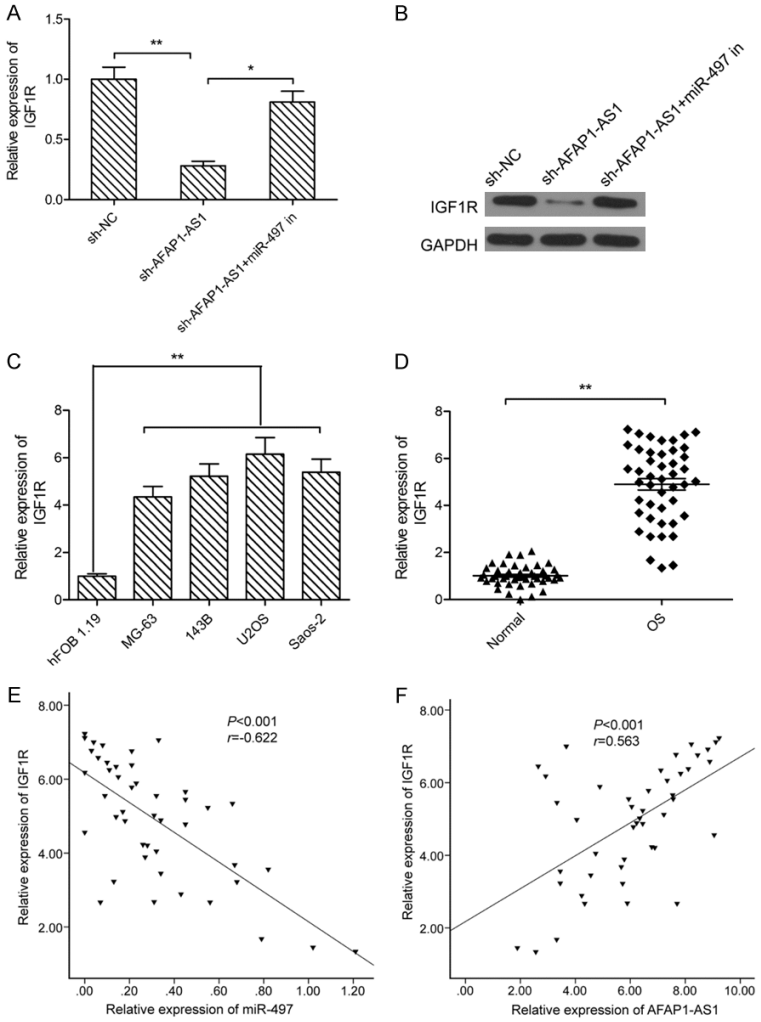

Figure 6. Associated role of AFAP1-AS1, miR-497 and IGF1R in OS progression. A, B. miR-497 inhibition reversed the reduction of IGF1R expression caused by AFAP1-AS1 knockdown in U2OS cells. C. The expression of *IGF1R* mRNA was upregulated in four human OS cell lines (MG-63, 143B, U2OS, Saos-2). D. The expression of *IGF1R* mRNA was upregulated in human OS tissues. E. Pearson correlation analysis revealed that there existed a negative association between *IGF1R* and miR-497 in OS tissues. F. Pearson correlation analysis revealed that there existed a positive association between *IGF1R* and AFAP1-AS1 in OS tissues. Data were presented as mean ± standard deviation (SD). Each experiment was repeated three times. *P < 0.05, **P < 0.01.

Discussion

A number of lncRNAs have been reported to be involved in the occurrence and development of OS, and function as tumor suppressors or proto-oncogenes in OS [10-12]. For example, Guan *et al.* reported that lncRNA APTR promoted OS progression through inhibition of miR-132-3p and upregulation of yes-associated protein 1 [28]. He *et al*. demonstrated that LINC00628 suppressed the growth and invasion through regulating PI3K/Akt signaling pathway in OS [29]. Ju *et al*. showed that SNHG5 aggravated the proliferation, migration and invasion of OS cells via the miR-212-3p/SGK3 axis [30]. Gu *et al*. revealed that HOXD-AS1 promoted OS carcinogenesis through epigenetically inhibiting p57 via EZH2 [31]. Therefore, it is significant to identify potential lncRNAs involved in OS progression. Here, we found that AFAP1-AS1 expression was upregulated in OS tissues and cell lines, which was consistent with previous studies [21, 22]. In addition, increased AFAP1-AS1 expression was closely associated with TNM stage, tumor size, metastasis and overall survival. Our study also showed that knockdown of AFAP1-AS1 inhibited OS cell proliferation, colony formation, migration and invasion and induced cell apoptosis *in vitro*, as well as retarded tumor growth *in vivo* by regulating miR-497/IGF1R. These finding suggested that AFAP1-AS1 might be an important prognostic factor and a potential therapeutic target for OS.

The AFAP1-AS1 was initially reported in esophageal adenocarcinoma in 2013 [32]. Recently, growing evidence has shown that AFAP1-AS1 played crucial roles in tumor progression in multiple cancers [13-20], suggesting that it might serve as a potential prognostic indica-

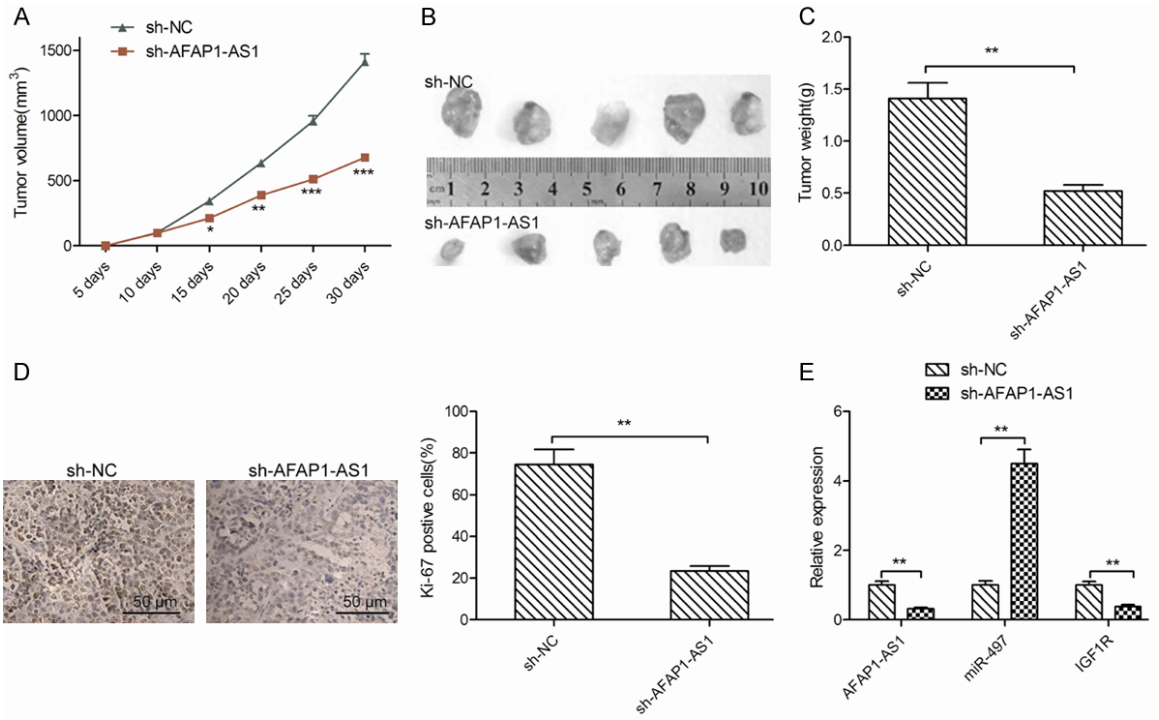

Figure 7. Knockdown of AFAP1-AS1 inhibited tumor growth *in vivo*. A. AFAP1-AS1 knockdown inhibited tumor growth *in vivo*. B. Representative images of formed tumors that were subcutaneously injected with U2OS cells stable transfected with sh-AFAP1-AS1 and sh-NC plasmid. C. Weight of formed tumors were decreased in AFAP1-AS1 depletion group. D. Ki-67 positive cells were decreased in tumor nodule tissues from AFAP1-AS1 depletion group. E. The expression of AFAP1-AS1, *IGF1R* were decreased and miR-497 expression were increased in tumor nodule tissues from AFAP1-AS1 depletion group. Data were presented as mean ± standard deviation (SD). Each experiment was repeated three times. **P* < 0.05, ***P* < 0.01.

tors and therapeutic targets in these cancers. Although recent studies have demonstrated that the AFAP1-AS1 implicated in OS progression [21, 22], the detail roles and underlying mechanisms of AFAP1-AS1 in OS remained largely unclear. In the present study, we found that AFAP1-AS1 was overexpressed in OS tissues and cell lines, which was consistent with previous results [21, 22]. Increased AFAP1-AS1 was positively associated with advanced TNM stage, metastasis, larger tumor size and poor overall survival. Loss-of-function experiments demonstrated that knockdown of AFAP1-AS1 inhibited OS cell proliferation, colony formation, migration and invasion, and induced cell apoptosis. Besides, we confirmed the functions of AFAP1-AS1 in OS *in vivo* by establishing nude mice models. These findings demonstrated that AFAP1-AS1 might play an oncogenic role in OS progression.

It is well known that lncRNAs exert their biological function through multiple ways among which acting as competing endogenous RNAs (ceRNAs) is an important path by sponging miRNAs [27, 33]. Several studies reported that AFAP1-AS1 could serve as ceRNAs by sponging miR-423-5p in nasopharyngeal carcinoma [14], miR-133a and miR-146-5p in pancreatic cancer [15, 34], miR-320a in laryngeal carcinoma [35]. To discover the potential molecular mechanisms by which AFAP1-AS1 serves as a ceRNA in OS progression. A bioinformatics analysis (StarBase2.0) showed that AFAP1-AS1 contains a potential binding site for miR-497. Moreover, miR-497 was reported to function as tumor suppressor in OS [24, 25]. Therefore, we speculated that AFAP1-AS1 may mediate OS progression by interacting with miR-497. Here, we found that miR-497 expression was downregulated in OS tissues and cell lines, which was consistent with previous reports [24, 25]. We also showed that miR-497 expression was negatively AFAP1-AS1 expression in OS tissues. Subsequently, luciferase reporter and anti-Ago2 RIP assays further confirmed that AFAP1-

AS1 directly targeted miR-497 in OS cells. In addition, the expression of miR-497 was negatively regulated by AFAP1-AS1 in OS cells. Meanwhile, miR-497 also negatively regulated AFAP1-AS1. Importantly, rescue experiments *in vitro* revealed that miR-497 inhibition reversed the inhibitory effects of AFAP1-AS1 knockdown in OS cells. These results indicated that AFAP1-AS1 promoted OS growth by sponging miR-497.

It has been shown that lncRNA function as ceRNA by sponging miRNAs, which can indirectly modulate the target gene expression of miRNAs [27, 36]. Recently a study demonstrated that miR-497 inhibited cell proliferation, migration and invasion in OS cell lines by IGF1R [25]. IGF1R was reportedly to function as an oncogene in multiple types of cancers including OS [37, 38]. Thus, the present study investigated that the association AFAP1-AS1, miR-497 and IGF1R in OS cells. Rescue experiments revealed that knockdown of AFAP1-AS1 significantly IGF1R expression, while miR-497 inhibitor could partially reversed this trend in U2OS cells. Moreover, we found that *IGF1R* mRNA expression levels were upregulated in OS tissues and cell lines. Pearson correlation analysis indicated that *IGF1R* expression was negatively correlated with miR-497 expression in OS tissues, and positively correlated with AFAP1-AS1 expression in OS tissues. These data suggested that AFAP1-AS1 promoted the tumorigenesis and progression of OS through competitively binding miR-497 and indirectly regulating IGF1R expression.

Conclusion

Taken together, the present study illustrated that AFAP-AS1 was a novel oncogene which promoted the tumorigenesis and progression of OS through competitively binding miR-497 and regulating IGF1R expression. This study suggested that AFAP1-AS1 might be a promising therapy target for the treatment of OS.

Disclosure of conflict of interest

None.

Address correspondence to: Mingzhu Xu, Department of Nephrology, The Third Hospital of Jilin University, Changchun 130033, P. R. China. E-mail: wenas12@sina.com; Yang Zhang, Department of Neurosurgery, The First Hospital of Jilin University, Changchun 130021, P. R. China. E-mail: zhangyangzy1020@sina.com

References

[1] Messerschmitt PJ, Garcia RM, Abdul-Karim FW, Greenfield EM and Getty PJ. Osteosarcoma. J Am Acad Orthop Surg 2009; 17: 515-527.

[2] Kager L, Zoubek A, Pötschger U, Kastner U, Flege S, Kempf-Bielack B, Branscheid D, Kotz R, Salzer-Kuntschik M, Winkelmann W, Jundt G, Kabisch H, Reichardt P, Jürgens H, Gadner H and Bielack SS; Cooperative German-Austrian-Swiss Osteosarcoma Study Group. Primary metastatic osteosarcoma: presentation and outcome of patients treated on neoadjuvant Cooperative Osteosarcoma Study Group protocols. J Clin Oncol 2003; 21: 2011-2018.

[3] Simpson S, Dunning MD, de Brot S, Grau-Roma L, Mongan NP and Rutland CS. Comparative review of human and canine osteosarcoma: morphology, epidemiology, prognosis, treatment and genetics. Acta Vet Scand 2017; 59: 71.

[4] Novikova IV, Hennelly SP, Tung CS and Sanbonmatsu KY. Rise of the RNA machines: exploring the structure of long non-coding RNAs. J Mol Biol 2013; 425: 3731-3746.

[5] Ponting CP, Oliver PL and Reik W. Evolution and functions of long noncoding RNAs. Cell 2009; 136: 629-641.

[6] Gutschner T and Diederichs S. The hallmarks of cancer: a long non-coding RNA point of view. RNA Biol 2012; 9: 703-719.

[7] Bartel DP. MicroRNAs: genomics, biogenesis, mechanism, and function. Cell 2004; 116: 281-297.

[8] Corra F, Agnoletto C, Minotti L, Baldassari F and Volinia S. The network of non-coding RNAs in cancer drug resistance. Front Oncol 2018; 8: 327.

[9] Balas MM and Johnson AM. Exploring the mechanisms behind long noncoding RNAs and cancer. Noncoding RNA Res 2018; 3: 108-117.

[10] Wang C, Jing J and Cheng L. Emerging roles of non-coding RNAs in the pathogenesis, diagnosis and prognosis of osteosarcoma. Invest New Drugs 2018; 36: 1116-1132.

[11] Smolle MA and Pichler M. The role of long noncoding RNAs in osteosarcoma. Noncoding RNA 2018; 4: 7.

[12] Kushlinskii NE, Fridman MV and Braga EA. Molecular mechanisms and microRNAs in osteosarcoma pathogenesis. Biochemistry (Mosc) 2016; 81: 315-328.

[13] Ji D, Zhong X, Jiang X, Leng K, Xu Y, Li Z, Huang L, Li J and Cui Y. The role of long non-coding

RNA AFAP1-AS1 in human malignant tumors. Pathol Res Pract 2018; 214: 1524-1531.
[14] Lian Y, Xiong F, Yang L, Bo H, Gong Z, Wang Y, Wei F, Tang Y, Li X, Liao Q, Wang H, Zhou M, Xiang B, Wu X, Li Y, Li X, Chen X, Li G, Guo C, Zeng Z and Xiong W. Long noncoding RNA AFAP1-AS1 acts as a competing endogenous RNA of miR-423-5p to facilitate nasopharyngeal carcinoma metastasis through regulating the Rho/Rac pathway. J Exp Clin Cancer Res 2018; 37: 253.
[15] Chen B, Li Q, Zhou Y, Wang X, Zhang Q, Wang Y, Zhuang H, Jiang X and Xiong W. The long coding RNA AFAP1-AS1 promotes tumor cell growth and invasion in pancreatic cancer through upregulating the IGF1R oncogene via sequestration of miR-133a. Cell Cycle 2018; 17: 1949-1966.
[16] He J, Wu K, Guo C, Zhou JK, Pu W, Deng Y, Zuo Y, Zhao Y, Liu L, Wei YQ and Peng Y. Long noncoding RNA AFAP1-AS1 plays an oncogenic role in promoting cell migration in non-small cell lung cancer. Cell Mol Life Sci 2018; 75: 4667-4681.
[17] Wang Y and Lan Q. Long non-coding RNA AFAP1-AS1 accelerates invasion and predicts poor prognosis of glioma. Eur Rev Med Pharmacol Sci 2018; 22: 5223-5229.
[18] Ma D, Chen C, Wu J, Wang H and Wu D. Up-regulated lncRNA AFAP1-AS1 indicates a poor prognosis and promotes carcinogenesis of breast cancer. Breast Cancer 2019; 26: 74-83.
[19] Tang J, Zhong G, Wu J, Chen H and Jia Y. Long noncoding RNA AFAP1-AS1 facilitates tumor growth through enhancer of zeste homolog 2 in colorectal cancer. Am J Cancer Res 2018; 8: 892-902.
[20] Dai W, Tian Y, Jiang B and Chen W. Down-regulation of long non-coding RNA AFAP1-AS1 inhibits tumor growth, promotes apoptosis and decreases metastasis in thyroid cancer. Biomed Pharmacother 2018; 99: 191-197.
[21] Zhao BM, Cheng FH and Cai L. Long noncoding RNA AFAP1-AS1 promoted osteosarcoma proliferation and invasion via upregulating BDNF. Eur Rev Med Pharmacol Sci 2019; 23: 2744-2749.
[22] Li R, Liu S, Li Y, Tang Q, Xie Y and Zhai R. Long noncoding RNA AFAP1-AS1 enhances cell proliferation and invasion in osteosarcomathrough regulating miR-4695-5p/TCF4-β-catenin signaling. Mol Med Rep 2018; 18: 1616-1622.
[23] Yang G, Xiong G, Cao Z, Zheng S, You L, Zhang T and Zhao Y. miR-497 expression, function and clinical application in cancer. Oncotarget 2016; 7: 55900-55911.
[24] Ge L, Zheng B, Li M, Niu L and Li Z. MicroRNA-497 suppresses osteosarcoma tumor growth in vitro and in vivo. Oncol Lett 2016; 11: 2207-2212.
[25] Liu Q, Wang H, Singh A and Shou F. Expression and function of microRNA-497 in human osteosarcoma. Mol Med Rep 2016; 14: 439-445.
[26] Tuo H, Wang Y, Wang L, Yao B, Li Q, Wang C, Liu Z, Han S, Yin G, Tu K and Liu Q. MiR-324-3p promotes tumor growth through targeting DACT1 and activation of Wnt/beta-catenin pathway in hepatocellular carcinoma. Oncotarget 2017; 8: 65687-65698.
[27] Salmena L, Poliseno L, Tay Y, Kats L and Pandolfi PP. A ceRNA hypothesis: the rosetta stone of a hidden RNA language? Cell 2011; 146: 353-358.
[28] Guan H, Shang G, Cui Y, Liu J, Sun X, Cao W, Wang Y and Li Y. Long noncoding RNA APTR contributes to osteosarcoma progression through repression of miR-132-3p and upregulation of yes-associated protein 1. J Cell Physiol 2019; 234: 8998-9007.
[29] He R, Wu JX, Zhang Y, Che H and Yang L. LncRNA LINC00628 overexpression inhibits the growth and invasion through regulating PI3K/Akt signaling pathway in osteosarcoma. Eur Rev Med Pharmacol Sci 2018; 22: 5857-5866.
[30] Ju C, Zhou R, Sun J, Zhang F, Tang X, Chen KK, Zhao J, Lan X, Lin S, Zhang Z and Lv XB. LncRNA SNHG5 promotes the progression of osteosarcoma by sponging the miR-212-3p/SGK3 axis. Cancer Cell Int 2018; 18: 141.
[31] Gu W, Zhang E, Song L, Tu L, Wang Z, Tian F, Aikenmu K, Chu G and Zhao J. Long noncoding RNA HOXD-AS1 aggravates osteosarcoma carcinogenesis through epigenetically inhibiting p57 via EZH2. Biomed Pharmacother 2018; 106: 890-895.
[32] Wu W, Bhagat TD, Yang X, Song JH, Cheng Y, Agarwal R, Abraham JM, Ibrahim S, Bartenstein M, Hussain Z, Suzuki M, Yu Y, Chen W, Eng C, Greally J, Verma A and Meltzer SJ. Hypomethylation of noncoding DNA regions and overexpression of the long noncoding RNA, AFAP1-AS1, in Barrett's esophagus and esophageal adenocarcinoma. Gastroenterology 2013; 144: 956-966, e954.
[33] Cheng DL, Xiang YY, Ji LJ and Lu XJ. Competing endogenous RNA interplay in cancer: mechanism, methodology, and perspectives. Tumour Biol 2015; 36: 479-488.
[34] Zhou J, Liu M, Chen Y, Xu S, Guo Y and Zhao L. Cucurbitacin B suppresses proliferation of pancreatic cancer cells by ceRNA: effect of miR-146b-5p and lncRNA-AFAP1-AS1. J Cell Physiol 2019; 234: 4655-4667.
[35] Yuan Z, Xiu C, Song K, Pei R, Miao S, Mao X, Sun J and Jia S. Long non-coding RNA AFAP1-AS1/miR-320a/RBPJ axis regulates laryngeal

carcinoma cell stemness and chemoresistance. J Cell Mol Med 2018; 22: 4253-4262.
[36] Giza DE, Vasilescu C and Calin GA. MicroRNAs and ceRNAs: therapeutic implications of RNA networks. Expert Opin Biol Ther 2014; 14: 1285-1293.
[37] Cao Y, Roth M, Piperdi S, Montoya K, Sowers R, Rao P, Geller D, Houghton P, Kolb EA, Gill J and Gorlick R. Insulin-like growth factor 1 receptor and response to anti-IGF1R antibody therapy in osteosarcoma. PLoS One 2014; 9: e106249.
[38] Schedlich LJ, Yenson VM and Baxter RC. TGF-beta-induced expression of IGFBP-3 regulates IGF1R signaling in human osteosarcoma cells. Mol Cell Endocrinol 2013; 377: 56-64.